Ind. J. Pharm. Edu. Res., 2027; 1-10.
https://www.ijper.org

Original Article

Cytotoxic Effects of Cyanidin Chloride in HepG2 Cells Associated with Altered LATS1 Gene Expression

Rashed M. Almuqbil*

Department of Pharmaceutical Sciences, College of Clinical Pharmacy, King Faisal University, Al-Ahsa, SAUDI ARABIA.

ABSTRACT

Background: Hepatocellular carcinoma (HepG2 cell line) is one of the major life-threatening cancers globally, leading to the need for identification of novel bioactive compounds with efficient anti–cancer activity. Cyanidin chloride, an anthocyanidin, belongs to the flavonoid family and has attracted interest since it has been reported to have anti-cancer potency against other cancers, whereas it is insufficiently studied in HepG2 cells. The objective of this investigation is to establish the anti-cancer activity of Cyanidin chloride against HepG2 cells. **Materials and Methods:** Cyanidin chloride was tested for its cytotoxicity against the HepG2 cell line by MTT assay. Apoptosis induction was assessed by Acridine orange/Ethidium bromide staining. Reactive oxygen species release and Mitochondrial membrane potential were analysed by DCFDA staining and the Mito Potential kit, respectively. Cell cycle and caspase-3 status were investigated by flow cytometry analysis and ELISA kit method, respectively. Molecular docking was performed for Cyanidin chloride Vs. LATS1 gene and the expression of the LATS1 gene was checked by quantitative PCR. **Results:** Cytotoxicity analysis revealed reduced cell viability of HepG2 in a concentration-dependent manner upon treatment with cyanidin chloride, and the IC50 value was obtained as 135.57 µg/mL. Acridine orange/Ethidium bromide staining showed an increased dead cell count in the treated group. Elevated intracellular reactive oxygen species liberation and marked alteration in the mitochondrial membrane potential were observed in the cyanidin-treated group. Cell cycle progression was distinct in the treated cells, and augmented caspase-3 levels were observed. LATS1 gene, one of the core factors in the Hippo signalling pathway, exhibited down-regulated gene expression in the treated group. Molecular docking analysis suggested the favourable binding of Cyanidin to the LATS1 protein, with a binding score of -7.4. **Conclusion:** Cyanidin chloride treatment showed appreciable anti-cancer and anti-proliferation effects towards the HepG2 cell line. Reactive oxygen species-associated mitochondrial membrane dysfunction, elevated caspase 3 release, and downregulated LATS1 gene expression collectively suggest the apoptotic progression of HepG2 cells. Cyanidin chloride is established as a promising anti-cancer drug for future use but warrants a deeper mechanistic evaluation of LATS1 protein activity and YAP phosphorylation in the Hippo signalling pathway.

Keywords: Anthocyanins, Cyanidin chloride, Hepatocellular carcinoma, HepG2 cells, Hippo signalling pathway, LATS1 gene.

Correspondence:
Dr. Rashed M. Almuqbil
Department of Pharmaceutical Sciences, College of Clinical Pharmacy, King Faisal University, Al-Ahsa 31982, SAUDI ARABIA.
Email: ralmuqbil@kfu.edu.sa

Received: 13-10-2026;
Revised: 18-10-2026;
Accepted: 26-10-2026.

www.ijper.org

INTRODUCTION

Hepatocellular Carcinoma (HCC) is a major global health burden, reported as the sixth most commonly diagnosed cancer among all cancers and ranking third in cancer-related mortality rate.[1,2] HCC development has a complex etiological factors and is associated with persistent hepatic injury arising from Hepatitis B and C viral infections, MAFLD – metabolic dysfunction-associated steatosis liver disease, MASH – metabolic dysfunction-associated steatohepatitis, triggered by hormonal imbalance and alcoholism etc.[3–6] Reports stated that alcohol-related HCC will rise from 19% to 21% and MASH- related HCC cases will be elevated from 8% to 11% by 2050.[7] 5-year survival of 40%–75% for patients with transplantation or resection in early-stage disease and 5%–13% survival among patients with locally advanced disease is dismal.[3] HCC incidence rate is higher in men than in women, reported as 2:1 or 4:1, reflecting the contribution of multiple biological and metabolic causative factors.[8,9] Failure in early diagnosis leads to the disease status worsening, while it is observed at advanced stages when curative interventions may no longer be feasible. There are many screening procedures available, like imaging, liquid biopsy, and pathology screenings, to determine the disease stage. Currently available treatments

DOI: 10.5530/ijper.20270907

Copyright Information :
Copyright Author (s) 2027 Distributed under Creative Commons CC-BY 4.0

Publishing Partner : Manuscript Technomedia. [www.mstechnomedia.com]

include surgical interventions, local ablative procedures, liver transplantation, radiotherapy, adjuvant therapies, chemotherapy, and trans arterial interventions, etc., depending on the stages of HCC. The worst part of the conventional treatment is cancer recurrence.[10–12] Many countries are working hard towards reducing the incidence rate, increasing surveillance facilities, and providing awareness of early diagnosis. Limitations in conventional therapies are shifting the concern towards the emergence of new therapeutic drugs with limited or no side effects. Naturally occurring plant-based bioactive molecules are the primary choices for anti-cancer candidates.

Polyphenols are gaining attention in recent days due to their diverse pharmacological benefits, including anti-cancer, antioxidant, anti-inflammatory, anti-microbial, anti–aging, anti–metastatic, etc., Among polyphenols, flavonoids constitute an important subgroup and have been extensively tested for their modulating impact on cancer cell progression and development. Anthocyanins (AC), a major category among flavonoid-derived pigments responsible for purple, red, and blue colours in fruits and vegetables, are directly absorbed and distributed to the blood. ACs are known as potent anti-oxidant due to its phenolic structure and hydroxyl groups.[13,14] Anthocyanidin possesses six major structurally derived compounds with pleiotropic effects on proliferation, oxidative stress, inflammation, and apoptosis, including cyanidin, pelargonidin, peonidin, malvidin, petunidin, and delphinidin.[1,15,16]

Cyanidin chloride is one of the important compounds known for its anti-microbial, anti-cancer, anti-inflammatory, and antioxidant properties.[17] Previous studies have reported that cyanidin chloride and its derivatives can modulate several cancer-associated signalling networks such as NF-kB, Wnt, and MAPK/JNK pathways, thereby influencing cellular survival and proliferation. Yeh and Yen (2005 demonstrated that cyanidin, malvidin, and delphinidin exhibited cytotoxic effects on HepG2 cells and also stated that caspase-3 increased and that Bcl-2 proteins were regulated through the oxidative stress-mediated apoptotic pathway. Impairment of oxidative conditions and mitochondrial dysfunction ultimately lead to cell apoptosis. In parallel with the oxidative stress-associated pathway, the dysregulation of the Hippo pathway is closely associated with hepatocarcinogenesis. This is the pivotal pathway responsible for cell proliferation, survival, regeneration and tumour progression.[18,19] which involves many key factors including MST1/2 kinases, LATS1/2 kinases, and YAP/TAZ downstream regulators. MTS1/2 kinase activates LATS1/2 kinase, which phosphorylates YAP and TAZ. Phosphorylated YAP remains in the cytoplasm (Hippo ON) and tends to restrict tumour growth, whereas unphosphorylated YAP proceeds with nuclear localisation and interacts with TEAD (Hippo OFF), leading to tissue growth.[20] LATS1 is a pivotal key factor in the Hippo pathway. The loss or impaired regulation of LATS1 has a major impact on YAP activity that contributes to liver tumourigenesis.[18,21,22]

The present study was designed to examine the anticancer activity of Cyanidin Chloride (CYN) against HepG2 cells by evaluating its cytotoxicity, morphological alterations, apoptosis, intracellular ROS generation, mitochondrial membrane potential, cell cycle progression, and caspase-3 levels. Although the anticancer effects of cyanidin and related anthocyanidins have been previously reported, their association with LATS1 gene expression in HepG2 cells remains insufficiently explored. To address this research gap, the present study additionally investigated LATS1 gene expression and performed molecular docking to explore the potential interaction of CYN with the LATS1-containing protein complex. Thus, the study aimed to provide additional insight into the cellular responses to CYN and the possible involvement of LATS1-associated molecular changes, without establishing a direct mechanistic link to Hippo pathway activity.

MATERIALS AND METHODS

Cell line

The cell line used in this study was the HepG2 cell line, known as a human hepatic carcinoma cell line, acquired from ATCC, USA. Cells were grown in 10 % Dulbecco's modified eagles' medium supplemented with Sodium bicarbonate and L glutamine. An antibiotic and Antimycotic combination solution was added to the medium to prevent contamination. The flask received was subcultured with the medium and kept at 60–70% confluency. The cells were collected and processed further for the assays.

Cyanidin chloride preparation

Cyanidin chloride (CYN) was purchased from Sigma. 1 mg of CYN was weighed and dissolved in 0.01% dimethyl sulfoxide solution to a 1 mg/mL stock concentration. The mixture was sonicated for uniform mixing, filtered through a syringe filter to ensure sterility, and stored for further use.

MTT assay

The cytotoxicity potency of CYN was analysed against the HepG2 cell line using the MTT assay protocol. To perform the assay, the cells were seeded into the 96-well cell culture plate at 5000 cells/well. The cells were incubated for 24 hr, then CYN at various concentrations was added to the respective wells in triplicate. A control well was kept, and CYN was added at 6.25, 12.5, 25, 50, and 100 µg/mL along with the complete media. The cells with the drug were incubated under the appropriate conditions. The effects on the cells were primarily analysed through inverted phase-contrast microscopy. The damaged, detached, and shrunken cells were identified through direct microscopic visualisation. The MTT assay was performed upon confirming the effects. The media

www.ijper.org

with CYN were aspirated and replaced with 5 mg/mL of MTT solution prepared in 1XPBS. The cells with the MTT solution were incubated for 2 – 4 hr in order to form the formazan crystals. Later, the bluish-purple coloured formazan crystals were dissolved using raw DMSO (0.2 mL/well. Then the results were read at 540 nm. The obtained value was used to calculate the % Viability. The IC_{50} value was calculated using ED50 PLUS V1.0 software.

% Viability = (Mean OD of sample/Mean OD of Control) X 100

Acridine orange/PI staining

HepG2 cells were seeded as per standard protocol. The cells were treated with the IC50 dosage of CYN (135.57 µg/mL) and incubated for 24 hr; the untreated group was also maintained. The treated and untreated cells were exposed to 100 µg/mL of Acridine Orange (AO) and Ethidium Bromide (EtBr) solution. The AO/EtBr exposed cells were incubated at room temperature for 10 min, followed by twice washing with 1X PBS. The stained cells were observed under fluorescence microscopy (Olympus CKX41 with Optika Pro5 camera) with a blue filter. The cells were categorised based on the fluorescence emission as follows: if the nucleus emits green fluorescence - living cells; bright green with fragmented chromatin – early apoptosis; orange emission with fragmented chromatin – late apoptosis; and orange emission – necrotic cells. 200 cells were arbitrarily counted and categorised into various cell phases. The cell numbers were converted to percentages and expressed in the results section.

DCFDA staining assay

Cells were treated with CYN (135.57 µg/mL) for 24 hr. The groups of treated and non-treated cells were subjected to the DCFDA staining protocol to assess reactive oxygen species release. Cells were exposed to 50 µl of DCFDA and incubated for 30 min. The unattached stains were removed through PBS (1X) washing. Then the stained cells were visualised under fluorescence microscopy (Olympus CKX41 with Optika Pro5 CCD camera) and measured using a fluorimeter (Qubit 3.0, Life Technologies, USA) at 470 nm and 635 nm excitation and emission wavelengths, respectively, expressed in arbitrary units. The results were not normalised to the control.

Mito potential assay

Cells of CYN (135.57 µg/mL) treated and untreated cells were collected by trypsinization and subjected to centrifugation to collect the cell pellet. Mito potential kit (Catalogue No. MCH100110) was used to determine the mitochondrial membrane potential. Mito potential dye was prepared at a 1: 1000 ratio using 1X assay buffer and labelled as the working solution. The obtained cell pellet was resuspended by 95 µL of Mito potential working solution and incubated for 20 min at 37 °C. Then, 5 µL of 7-AAD dye was added to the solution, mixed by gentle up-and-down pipetting, and incubated at 37 °C for 5 min. The samples of treated and untreated cells were loaded into the flow cytometer (Millipore, USA), and the events were obtained after completing the gating strategies with respect to control cells.

Cell cycle assay

CYN (135.57 µg/mL) treated and control cells were trypsinized and centrifuged to obtain the cell pellet. Then the cells were washed twice with 1X PBS by centrifugation at 3000 rpm for 5 min. Cells were counted using a hemocytometer to maintain the standard cell count ($1x10^6$ cells) for cell cycle analysis. The fixed cell count was taken in the fresh tube and washed again with 1X PBS for the complete removal of residual FBS. Then, 70% ice-cold ethanol was added dropwise to the pellet with tapping to prepare the single-cell suspension. The cells with the ethanol were incubated at 4 °C overnight. The cells were centrifuged to remove the ethanol and then washed with PBS. 250 µL of cell cycle reagent was added and incubated for 30 min in the dark, then subjected to flow cytometry analysis after gating strategies were performed with respect to the control group.

Caspase 3 assay

Cells were treated with CYN (135.57 µg/mL) at sufficient confluency, and the untreated group was also maintained. 100 µL of supernatant was taken from the respective treated and untreated groups and added to a 96-well plate and incubated overnight at 37 °C. The wells were drained and washed with PBS twice. Then 200 µL of blocking buffer (0.2% gelatine in 0.05% Tween 20: Merck; Germany prepared in PBS) was added and incubated for 60 min at room temperature. Then washed with PBS TWEEN. Caspase 3 – primary antibody (Santacruz, 1:500) 100 µL was introduced into each and every well, incubated for 2 hr at room temperature then washed with PBS TWEEN twice. 100 µL of secondary antibody (HRP Conjugate, Santacruz, USA) was added and kept for 1 hr undisturbed at room temperature. It was then washed with PBS Tween twice. 200 µL of O-dianizdine hydrochloride (21 mL of citrate buffer (pH 5), 1mg/100 mL of methanol with 60 mL of H_2O_2: Sigma Aldrich, USA) was added and left for 30 min at room temperature. The reaction was stopped by adding 5N HCl (50 µL). Absorbance was read at 415 nm in an ELISA reader. The concentration of protein was also estimated (Bradford method).

The caspase-3-associated immunoreactive signal was measured by indirect ELISA, and absorbance was recorded at 415 nm. Total protein concentration was estimated using the Bradford method. The absorbance values were normalised to protein concentration and expressed as relative caspase-3-associated immunoreactivity (OD/protein concentration). This measurement represents a protein-normalised antibody-associated signal rather than caspase-3 enzymatic activity.

www.ijper.org

Molecular Docking: Retrieval and preparation of the LATS1 receptor

Molecular docking was performed to investigate the possible interaction of CYN with LATS1, a key component of the Hippo signalling pathway. The experimentally determined human MOB1A–LATS1 complex (PDB ID: 5BRK) was retrieved from the Protein Data Bank. The crystallographic resolution was 2.30 Å, and it contains the MOB kinase activator as chain A (MOB1A) and a LATS1 fragment as chain B. The receptor structure was prepared by removing crystallographic water molecules and non-structural heteroatoms, followed by conversion of the cleaned protein structure into PDBQT format. Polar hydrogens and Gasteiger partial charges were incorporated during receptor preparation. The prepared receptor contained 4,183 atoms and 255 unique residues according to the docking workflow used in the present study. A docking grid was defined with a center at x = 23.764, y = 37.244 and z = 9.810 Å, with dimensions of 20 × 20 × 20 Å and a grid spacing of 0.375 Å, corresponding to 40 × 40 × 40 grid points. CYN was subsequently docked against the prepared LATS1-containing receptor using AutoDock Vina, which ranks predicted ligand conformations according to its scoring function, with lower predicted binding free-energy values representing more favourable calculated binding poses.

Real-time PCR

The total RNA was isolated from the CYN (135.57 µg/mL) treated and untreated group using TRIzol reagent (Invitrogen – Product code 10296010). In brief, the cells were exposed to TRIzol reagent and centrifuged. The pellet was resuspended in chloroform,

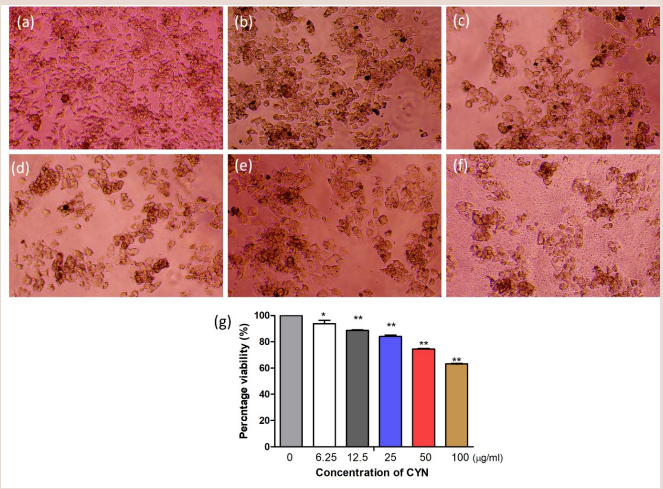

Figure 1: MTT assay: Cytotoxicity assessment of CYN against HepG2 cell line was performed. (a) – Control, (b) - 6.25, (c) - 12.5, (d) - 25, (e) 50 and (f) 100 µg/mL. (g) – denotes the graphical representation of percentage viability upon treated with various concentrations of CYN. One-way ANOVA was used for the statistical analysis, and treated groups were compared with the control groups through Tukey's multiple comparison test. $p<0.05$ is considered significant. * $p<0.05$, ** $p<0.01$.

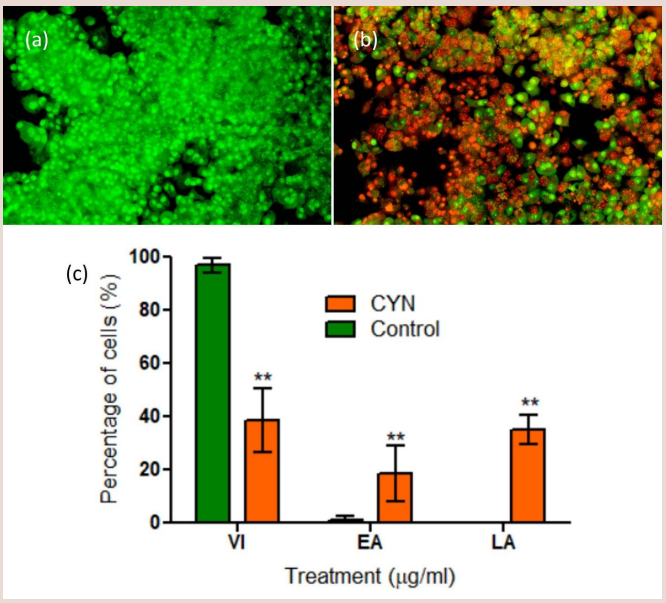

Figure 2: Acridine Orange/Ethidium bromide staining: Acridine Orange/Ethidium Bromide staining was performed to observe the apoptosis percentage upon treated with CYN against HepG2 cells. (a) – represents the increased live cells, and (b) - represents the equal viable and dead cells in the CYN-treated group. (c) – denotes the graphical representation of the percentage of cells in different apoptosis stages. One-way ANOVA was used for the statistical analysis, and treated groups were compared with the control groups through Tukey's multiple comparison test. $p<0.05$ is considered significant. ** $p<0.01$.

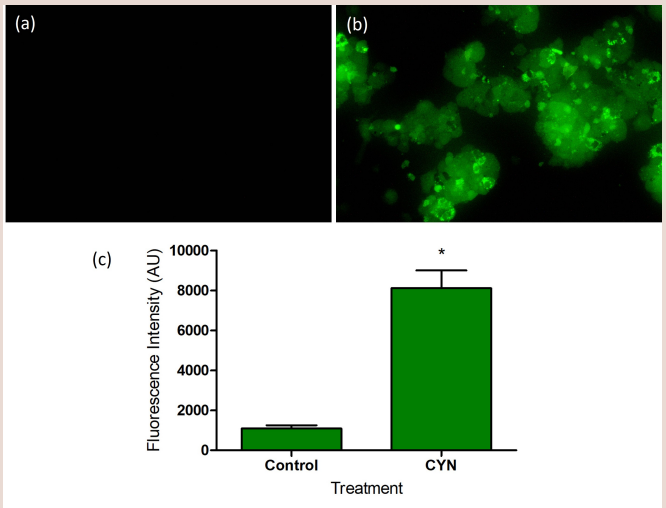

Figure 3: DCFDA staining assay. ROS release was determined by the DCFDA staining procedure. The figure showed the absence of green fluorescence in the control group depicted in (a) and increased green fluorescence in the CYN-treated group depicted in (b). The fluorescence intensity is expressed as arbitrary units in (c). One-way ANOVA was used for the statistical analysis, and treated groups were compared with the control groups through Tukey's multiple comparison test. $p<0.05$ was considered significant. * $p<0.05$.

www.ijper.org

followed by centrifugation. The aqueous layer was collected in a new tube and added to absolute isopropanol. The contents were centrifuged and washed with 75% ethanol twice. The final RNA pellet was dried and suspended in TE buffer. Quantitative and qualitative assessments were performed. The isolated RNA pellet was used as a template for cDNA synthesis using the iScript cDNA Synthesis Kit (Bio-Rad, Cat# 1708891 master premix for first-strand cDNA synthesis) as per the manufacturer's procedure. The optimal conditions used were given in Table 1. Synthesised cDNA was used as a template for real-time PCR experiments using SYBR Green Master Mix (G BIOSCIENCES, Product code-786-5062) using LightCycler 96 (Roche). All reactions were performed in triplicates and data were analysed according to $\Delta\Delta C_t$ method (using Light Cycler 96 SW 1.1 Software). The conditions used were tabulated as Table 2. LATS1 gene expression was analyzed in the treated and untreated groups, and GAPDH gene was used as a housekeeping gene. The primer sequence was tabulated as Table 3.

Statistical Analysis

One-way Analysis of Variance (ANOVA) was employed to assess the significance of differences between the control and treated groups. Tukey's multiple comparisons test was used to demonstrate comparisons between groups. Statistical analysis was performed using GraphPad Prism software, version 5.1. All assessments were triplicated, and data were submitted as mean ± SD. $p<0.05$ is considered significant for all experiments. ($n=3$; biological replicates).

Table 1: cDNA synthesis conditions.

Step	Temp. °C	Time (min)	No. of cycles
Priming	25	5	1
cDNA synthesis	46	20	1
Inactivation	95	1	1

RESULTS

MTT assay

Cytotoxicity assay was performed using MTT reagent for CYN-treated and untreated cells. The effect of CYN at various concentrations against the HepG2 cell line was revealed in Figure 1. Control cells showed distinct architecture in Figure 1(a), whereas the CYN-treated cells in Figure 1 (b – f) showed a progressive effect related to the increased dosages. Figure 1(g) depicts the graphical representation of the percentage of cell viability. The high dosage of 100 µg/mL exhibited 63.128 ± 0.171 % cell viability. IC50 value was calculated as 135.57 µg/mL using ED50 PLUS V1.0 Software. All the groups exhibited a moderate significant difference compared with the control group with ** ($p< 0.01$), except the 6.25 µg/mL group, which showed significance at $p< 0.05$.

Table 2: qPCR optimal conditions.

Steps	Time required	Temperature
Initial activation step	2 min	95°C
3 step cycling		
Denaturation	10 sec	95°C
Annealing	1 min	58°C
Extension	1 min/kb	72°C
Number of cycles	40 cycles	
End of PCR cycling	Indefinite	4°C

www.ijper.org

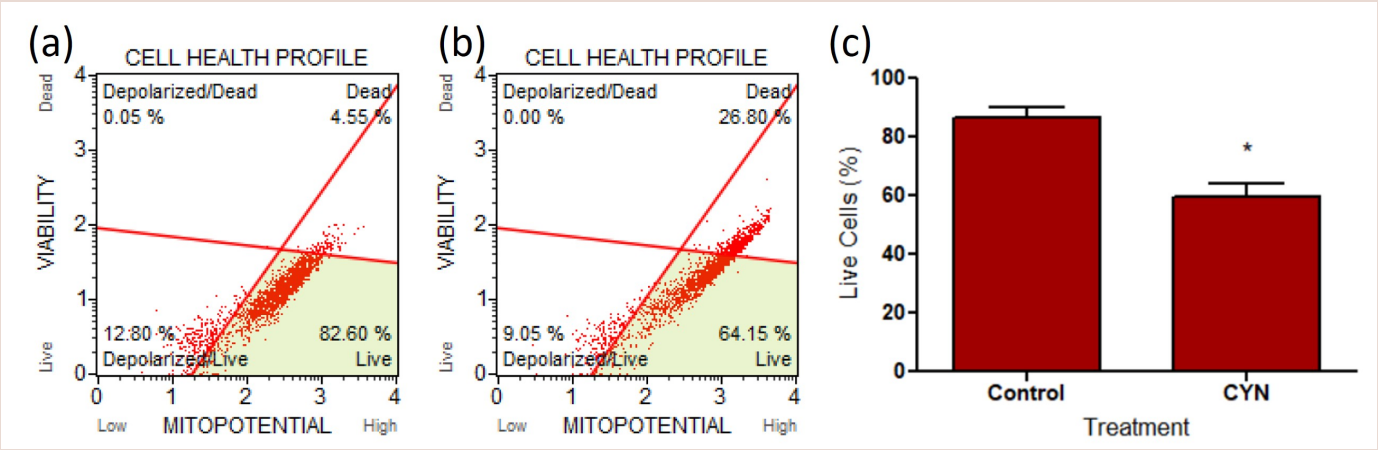

Figure 4: MMP assay. Mitochondrial membrane potential was assessed using the Muse Mito Potential Kit. (a) and (b) represent the health profile of cells in the control and treated groups, respectively. (c) – represents the graphical representation of the percentage of viable cells in the treated and control groups. One-way ANOVA was used for the statistical analysis, and treated groups were compared with the control group through Tukey's multiple comparison test. $p<0.05$ was considered significant. *$p<0.05$.

Acridine orange/EtBr

Acridine orange/Ethidium Bromide staining assay was performed to understand the status of apoptosis upon treatment with CYN. Untreated cells were also subjected to this experiment, which showed the maximum percentage of viable cells depicted in Figure 2 (a). CYN (IC50 – 135.57 µg/mL) treated group exhibited mixed fluorescence of green, bright green, and orange, indicating viable cells, early apoptotic cells, and late apoptotic cells, respectively, as shown in Figure 2 (b). The estimated cell percentage in each stage was represented as a graph in Figure 2 (c). Control/untreated cells showed an absence of early and late apoptosis, with 97 ± 2.82% viable cells. The treated group demonstrated 38.5 ± 12.02 % of viable cells, 18.5 ± 10.6% of early apoptotic cells, and 35 ± 5.65 % of late apoptotic cells. All the stages of treated groups exhibited a moderately significant difference compared with the control group, shown as ** $p< 0.01$.

DCFDA assay

Reactive Oxygen Species (ROS) liberation was tested for untreated and CYN-treated groups using the DCFDA staining method. Figure 3 (a) and (b) denote the DCFDA-stained control and treated cells, respectively. The green fluorescence emission was lower in the control group, showing 1089.5 ± 232.63 AU, which was elevated in the treated group to 8110 ± 1268.5 AU. From the graphical representation in Figure 3 (c), the augmented ROS liberation in the treated group was observed with a low significance difference compared with the control group * $p< 0.05$.

Mito potential assay

Mitochondrial membrane potential was assessed in the control and CYN-treated cells. The results of the cell health profile for the control and treated groups were shown in Figure 4 (a) and (b), respectively. Figure 4 (c) demonstrated the graphical representation of cell status, where the live cell percentage decreased to 59.37 ± 6.75 upon treatment with CYN; the control exhibited 86.37 ± 5.33 %. The treated group showed a low-significance difference compared with the control group, as indicated by* $p< 0.05$.

Cell cycle assay

Cell-cycle analysis revealed alterations in the distribution of HepG2 cells following CYN treatment (Figure 5c). In the control group, 63%, 12%, and 25% of cells were distributed in the G0/G1, S, and G2/M phases, respectively. Following CYN treatment, the G0/G1 population increased to 69%, whereas the S-phase population decreased to approximately 10%. The G2/M population also decreased to 18%. Statistically significant differences were observed in the G0/G1 and S phases compared with the control group ($p < 0.05$). These findings indicate changes in cell-cycle distribution following CYN treatment; however, they do not conclusively establish a specific cell-cycle arrest.

Caspase 3 assay

The CYN-treated and untreated groups were subjected to an assay to estimate caspase 3 activity. Figure 6 indicates the caspase 3 activity in both groups. The control group showed lower Caspase 3 activity (0.3635 ± 0.007), which was elevated in the CYN-treated group to 0.914 ± 0.22. Caspase 3 activity showed a reduced but significant difference compared with the control * $p< 0.05$.

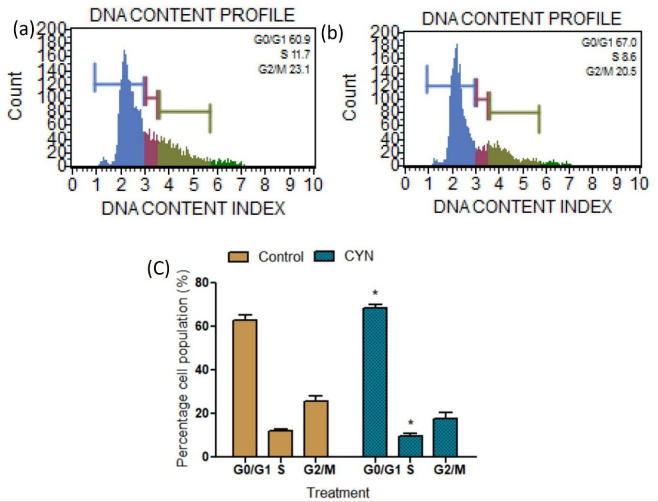

Figure 5: Cell cycle analysis. Cell cycle analysis was performed to understand the proliferation status of the cells in each cell cycle phase. (a) and (b) represent the cells in different stages of the cell cycle in the control and CYN-treated groups, respectively. (c) – denotes the graphical representation of cell population percentage in all the stages of both the treated and untreated groups. One-way ANOVA was used for the statistical analysis, and treated groups were compared with the control groups through Tukey's multiple comparison test. $p<0.05$ is considered significant. *$p<0.05$.

Table 3: Sequence of primers.

Gene names	FORWARD	Tm	REVERSE	Tm
LATS1	CACTGGCTTCAGATGGACACAC	62.1	GGCTTCAGTCTGTCTCCACATC	62.1
GAPDH	CACATCGCTCAGACACCATG	56.0	TGACGGTGCCATGGAATTTG	56.1

www.ijper.org

Molecular Docking

Molecular docking analysis demonstrated interaction between CYN and the LATS1-containing receptor structure. Among the generated conformations, the highest-ranked docking pose (Mode 1) exhibited a predicted binding affinity of −7.4 kcal/mol. The negative docking score indicates a favourable calculated energetic interaction between CYN and the receptor in the predicted binding configuration. Residue-contact analysis identified 13 amino acid residues located within 4.0 Å of the docked ligand. These residues comprised Ala44, Trp56, Val59, Asn60, Val62, Asp63, Asn66 and His185 from chain A, together with His646, Val650, Ser653, His654 and Arg657 from chain B. The two-dimensional interaction analysis showed the ligand positioned within a residue-rich binding environment involving several polar and non-polar amino acid residues, while the corresponding three-dimensional representation demonstrated that CYN was accommodated within the local protein surface (Figure 7).

Real time PCR

Quantitative real-time PCR analysis revealed a modest reduction in LATS1 mRNA expression in CYN-treated HepG2 cells compared with the untreated control group. The relative expression level was 0.786 ± 0.077-fold, corresponding to approximately 21.4% lower expression ($p < 0.05$). Although statistically significant, the magnitude of this change was relatively small. Therefore, these findings indicate an association between CYN treatment and altered LATS1 transcript abundance but do not establish changes in LATS1 protein expression, kinase activity, or downstream Hippo signalling (Figure 8).

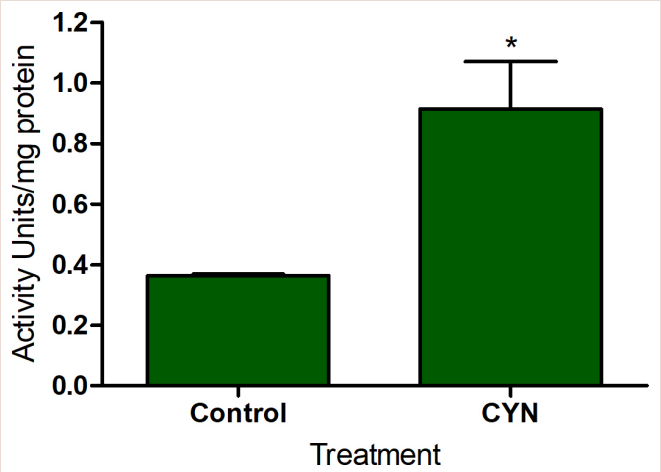

Figure 6: Caspase 3 assay. Caspase 3 was estimated for the CYN-treated group and control group; the results are depicted graphically in the figure and expressed as Activity Units/mg of protein. One-way ANOVA was used for the statistical analysis, and treated groups were compared with the control groups through Tukey's multiple comparison test. $p<0.05$ was considered significant. *$p<0.05$.

DISCUSSION

HCC is the predominant cancer worldwide; the incidence rate is increasing progressively. Hence, there is an urge to find a plant-based drug candidate instead of the already available conventional therapy, which has many side effects. The present study demonstrates that CYN exerts cytotoxic potency against HepG2 cells, accompanied by ROS release, MMP dysfunction, caspase 3 elevation, and altered LATS1 gene expression associated with the Hippo pathway.

HepG2 cell viability reduction was observed in the cytotoxicity assay, indicating the anti-proliferative efficacy of CYN. The morphological alterations also supported the results, demonstrating cell shrinkage, cell blubbing, and cell detachment in relation to the increasing dosage of CYN. The same morphological alterations were reported by Divya *et al.*, 2016 in HepG2 cells upon treatment with the anthocyanidins such as Malvidin (MAL) and Pelargonidin (PEL).[15] Anti-cancer potency of CYN was studied in a colon cancer cell line; Lee *et al.* (2020 reported dose-related apoptosis percentage through the Nrf2 and NF-κB pathways.[23] AO/EtBr apoptotic staining further supported the cytotoxicity outcomes, as it exhibited an increased proportion of dead cells with altered morphological characteristics in the CYN-treated group. The significant reduction of cell viability is consistent with the previous study reported by Yeh and Yen, 2005. The study reported that delphinidin, malvidin, and cyanidin exhibited growth-inhibitory effects against HepG2 cells.[16] Another study reported that the cytotoxicity of delphinidin against HepG2 cells exhibited 50 % cell death at 50 µg/mL, along with an increase in cleaved caspase 3.

The fluorescence staining with DCFDA exhibited elevated reactive oxygen species release in the CYN-treated group, indicating an imbalance in oxidative homeostasis. In cancer cells, excessive ROS liberation is a major cause of the impairment of numerous cellular functions. The loss of redo equilibrium and free electron radicals disturbs almost every cellular function, leading to mitochondrial membrane potential loss and subsequent activation of cytochrome c release, which tends to activate the caspase cascade-associated apoptosis pathway. Caspase 3 estimation also resulted in augmented caspase 3 activity; increased caspase 3 expression further confirms apoptosis. The combined findings of ROS and MMP suggest that MMP dysfunction and excessive ROS liberation, reflected in the Caspase 3 level, indicate the apoptotic direction of cancer cells.[24] To define the exact pathway, direct assessment of cytochrome C, apoptosis-related genes, and Caspase-9 expression would be required to establish the complete pathway conclusion. Studies have proven that anthocyanins possess strong free radical scavenging and antioxidant activity.[24,25] Quercetin, a flavonoid, exhibited excessive ROS release followed by mitochondrial depolarization

www.ijper.org

and sequential processes of caspase 3 and 9 elevation in the HepG2 cell line, as reported by Granado-Serrano *et al.*, 2006.[26]

Interestingly, CYN treatment did not produce a significant alteration in cell-cycle distribution. This observation suggests that the reduction in cell viability observed in the present study was not primarily dependent on a detectable cell-cycle arrest. This distinction is relevant because several anticancer compounds can reduce tumour-cell proliferation either by inducing cell-cycle blockade or by directly promoting programmed cell death. The absence of cell-cycle arrest should therefore not be interpreted as an absence of an antiproliferative effect, but rather as evidence that the cytotoxic response under the experimental conditions employed was more closely associated with cell death than with accumulation of cells at a particular cell-cycle phase. A similar discussion between growth inhibition, apoptosis and cell-cycle progression has been reported in HepG2 cells treated with gallic acid, where reduced cell growth and increased apoptosis occurred without significant interference with cell-cycle progression.[27]

The docking result provides computational evidence that CYN can adopt a stable and energetically favourable pose within the selected region of the human MOB1A–LATS1 receptor structure. The predicted affinity of −7.4 kcal/mol, together with the involvement of multiple residues surrounding the ligand, suggests that several non-covalent interactions may contribute to stabilisation of the predicted complex. In particular, the presence of polar residues such as Asn60, Asp63, Asn66, Ser653 and Arg657, together with aromatic and hydrophobic residues including Trp56, Val59, Val62 and Val650, indicates a chemically diverse interaction environment capable of accommodating the hydroxyl-rich structure of CYN. However, the docking findings support the possibility of a direct molecular association between CYN and the LATS1-containing complex, but functional experiments are required to establish the biological consequence of this interaction.

The docking observation is particularly relevant to the present experimental finding of altered LATS1 gene expression following CYN treatment. The downregulated expression of the LATS1 gene indicates a transcriptional alteration involving a key component of the Hippo pathway; however, its functional significance in relation to the observed apoptotic effects remains unclear. The Hippo pathway is a highly conserved signalling cascade that regulates a broad range of biological processes, including tissue homeostasis, differentiation, cell survival, organ size, and tumour progression, through a group of key regulatory proteins.[18,28,29] LATS1 is a core component of the Hippo signalling pathway and functions as a tumour-suppressive serine/threonine kinase that regulates the downstream transcriptional coactivators YAP and TAZ. In the canonical Hippo pathway, activation of MST1/2 promotes LATS1/2 activation, followed by YAP/TAZ phosphorylation. Phosphorylated YAP is generally retained in the cytoplasm and/or targeted for degradation, thereby restricting YAP/TAZ-dependent transcriptional programs involved in cellular growth and survival. In hepatocarcinogenesis, dysregulation of the Hippo–YAP pathway contributes to tumour progression, as reduced LATS1 activity may permit increased YAP/TAZ-mediated oncogenic signalling.[22,30] Therefore, the reduced LATS1 mRNA expression observed in the present study cannot be

www.ijper.org

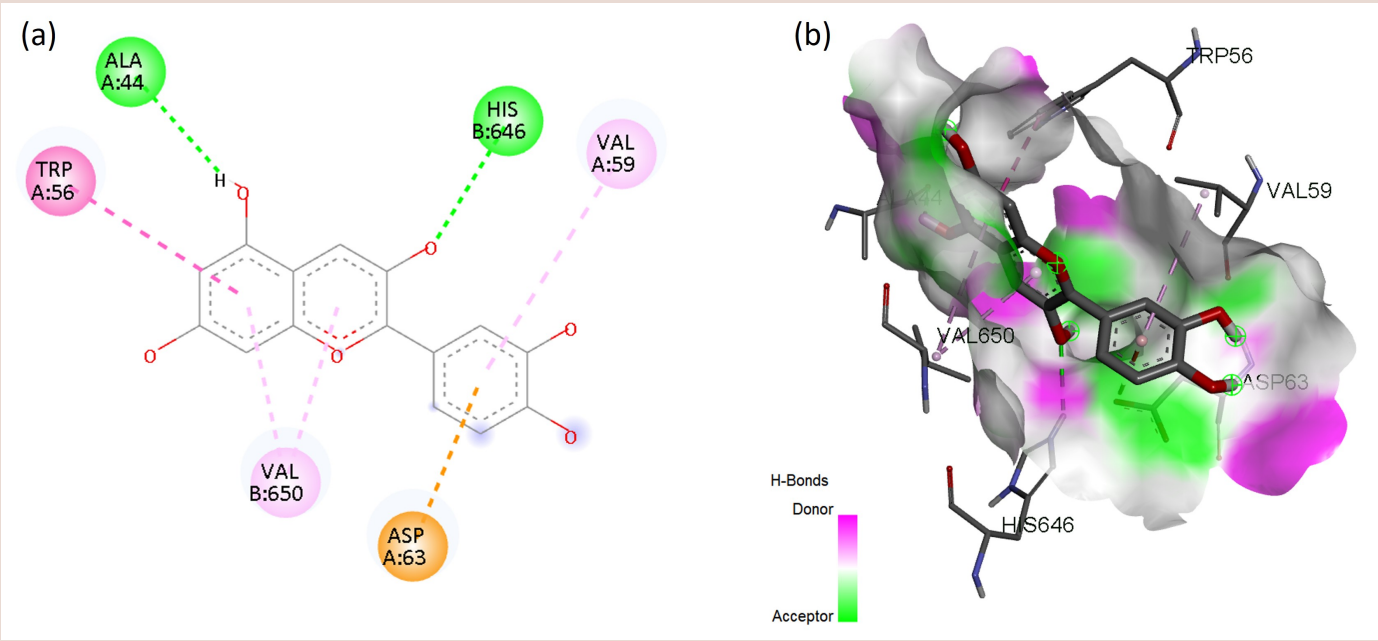

Figure 7: Molecular docking. Docking studies were performed to determine the binding affinity between the LATS1 gene and the CYN molecule. (a) and (b) represent the 2D and 3D docking outputs.

directly interpreted as a mechanism responsible for the anticancer activity of CYN. The observed transcriptional alteration may represent a secondary response associated with cellular stress or apoptotic progression; however, this possibility requires experimental confirmation. Furthermore, LATS1 mRNA expression does not necessarily reflect its protein abundance or kinase activity, and the present study did not evaluate LATS1 protein expression, YAP/TAZ phosphorylation, or downstream signalling activity. Previous studies have demonstrated the involvement of Hippo-associated signalling in the biological effects of natural compounds. Lorthongpanich *et al.* (2021) reported that the flavonoid fisetin suppressed YAP-associated signalling in mesenchymal stem cells,[31] whereas Li *et al.* (2018) demonstrated that decursin inhibited HepG2 cell proliferation through Hippo/YAP-associated mechanisms involving increased LATS1 phosphorylation and YAP degradation.[32] These findings highlight the importance of Hippo–YAP signalling in regulating cellular responses but do not establish a similar mechanism for CYN. Therefore, further investigations involving LATS1 protein expression and activity, YAP/TAZ phosphorylation, and downstream signalling are necessary to clarify the biological significance of LATS1 downregulation following CYN treatment.

Overall, the findings in the present study provide experimental evidence that CYN possesses a cytotoxic effect against HepG2 cells and suggest that oxidative stress-associated mitochondrial dysfunction and parallel alterations in LATS1 expression provide a potentially relevant molecular observation linking CYN treatment to Hippo-associated signalling and warrant further investigation.

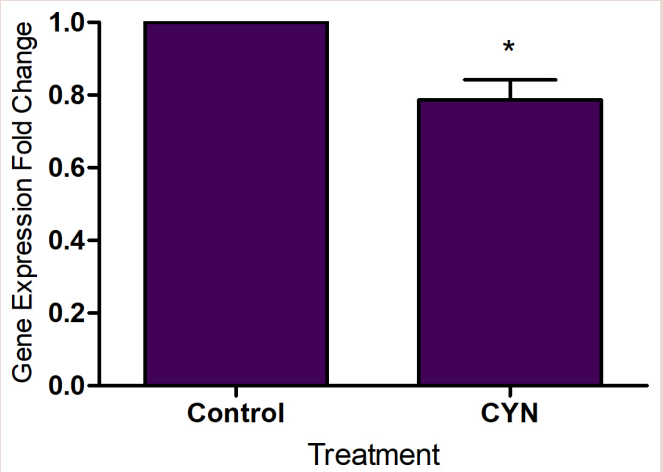

Figure 8: Real time PCR: Gene expression analysis was performed for the LATS1 gene in the CYN-treated group and untreated group, expressed as fold changes with respect to the housekeeping gene GAPDH. One-way ANOVA was used for the statistical analysis, and treated groups were compared with the control groups through Tukey's multiple comparison test. $p<0.05$ was considered significant. *$p<0.05$.

CONCLUSION

Collectively, the present findings demonstrated that CYN exposure reduced cell viability, increased intracellular ROS, which is associated with mitochondrial membrane depolarization and subsequent increased caspase-3 expression and apoptotic morphological changes. The absence of significant cell-cycle arrest further suggests that apoptosis rather than cell-cycle blockade represents the predominant response under the experimental conditions. In parallel, CYN treatment altered LATS1 gene expression, suggesting possible modulation of Hippo-associated signalling, but further protein expression studies are needed. Overall, the present findings provide experimental evidence that CYN possesses cytotoxic and pro-apoptotic activity against HepG2 cells and suggest oxidative stress-associated mitochondrial dysfunction. The concomitant alteration of LATS1 expression provides a potentially relevant molecular observation linking CYN treatment to Hippo-associated signalling and warrants further investigation. In addition, further investigations using additional cancer cell lines, non-malignant hepatic cells, and appropriate *in vivo* models are required to establish its selectivity, safety, and potential therapeutic relevance.

ACKNOWLEDGEMENT

I thank the Deanship of Scientific Research, Vice Presidency for Graduate Studies and Scientific Research, King Faisal University, Saudi Arabia, for their financial support.

ABBREVIATIONS

AC: Anthocyanins; **AO:** Acridine Orange; **ANOVA:** Analysis of Variance; **ATCC:** American Type Culture Collection; **CYN:** Cyanidin Chloride; **DCFDA:** 2′,7′-Dichlorodihydrofluorescein Diacetate; **DMSO:** Dimethyl Sulfoxide; **ELISA:** Enzyme-Linked Immunosorbent Assay; **EtBr:** Ethidium Bromide; **FBS:** Fetal Bovine Serum; **GAPDH:** Glyceraldehyde-3-Phosphate Dehydrogenase; **HCC:** Hepatocellular Carcinoma; **HRP:** Horseradish Peroxidase; **IC_{50}:** Half-Maximal Inhibitory Concentration; **LATS1:** Large Tumor Suppressor Kinase 1; **MAFLD:** Metabolic Dysfunction-Associated Fatty Liver Disease; **MAPK:** Mitogen-Activated Protein Kinase; **MASH:** Metabolic Dysfunction-Associated Steatohepatitis; **MMP:** Mitochondrial Membrane Potential; **MST1/2:** Mammalian Sterile 20-Like Kinases 1 and 2; **MTT:** 3-(4,5-Dimethylthiazol-2-yl)-2,5-Diphenyltetrazolium Bromide; **NF-κB:** Nuclear Factor Kappa B; **PBS:** Phosphate-Buffered Saline; **PCR:** Polymerase Chain Reaction; **qPCR:** Quantitative Polymerase Chain Reaction; **ROS:** Reactive Oxygen Species; **SD:** Standard Deviation; **TAZ:** Transcriptional Coactivator with PDZ-Binding Motif; **TEAD:** TEA Domain Transcription Factor; **YAP:** Yes-Associated Protein; **7-AAD:** 7-Aminoactinomycin D.

www.ijper.org

FUNDING

This work was funded through the Deanship of Scientific Research, Vice Presidency for Graduate Studies and Scientific Research, King Faisal University, Al-Ahsa, Saudi Arabia [Grant Number KFU266000].

CONFLICT OF INTEREST

The authors declare that there is no conflict of interest.

ETHICAL APPROVAL

There is no need for ethical approval for this project

AUTHORS CONTRIBUTION

Rashed M. Almuqbil: Conceptualization, Methodology, Investigation, Formal analysis, Data curation, Validation, Visualization, Writing – original draft, Writing – review and editing, Supervision, and Project administration.

SUMMARY

This study investigated the anticancer potential of cyanidin chloride against hepatocellular carcinoma (HepG2) cells, focusing on apoptosis and LATS1 gene expression associated with the Hippo signalling pathway. Cyanidin chloride exhibited concentration-dependent cytotoxicity, with an IC50 value of 135.57 µg/mL. Acridine orange/ethidium bromide staining confirmed increased apoptotic cell populations. Treatment significantly elevated intracellular reactive oxygen species, disrupted mitochondrial membrane potential, and increased caspase-3 activity, suggesting oxidative stress-associated mitochondrial apoptosis. Cell cycle analysis revealed no substantial cell cycle arrest, indicating that cytotoxicity was predominantly associated with apoptotic cell death. Molecular docking demonstrated favourable predicted binding of cyanidin chloride to the LATS1-containing protein complex, with a binding affinity of −7.4 kcal/mol. Quantitative PCR revealed significant downregulation of LATS1 gene expression. Collectively, these findings suggest that cyanidin chloride exhibits anticancer activity in HepG2 cells through apoptosis-associated mechanisms, accompanied by alterations in Hippo pathway-related signalling that warrant further mechanistic investigation and experimental validation.

REFERENCES

1. Sun S, Xu K, Yan M, *et al.* Delphinidin induces autophagic flux blockage and apoptosis by inhibiting both multidrug resistance gene 1 and DEAD-box helicase 17 expressions in liver cancer cells. J Pharm Pharmacol. 2023;75:253-63.
2. Singh SP, Madke T, Chand P. Global epidemiology of hepatocellular carcinoma. J Clin Exp Hepatol. 2025;15. doi:10.1016/j.jceh.2024.102446.
3. Anders R, Valero III V, Pawlik T. Emerging role of Hpo signaling and YAP in hepatocellular carcinoma. J Hepatocell Carcinoma. 2015;2:69.
4. Lee YT, Wang JJ, Danpanichkul P, *et al.* Recent trends of incidence, mortality, treatment, and overall survival of hepatocellular carcinoma in the United States. Clin Gastroenterol Hepatol. 2026;24:2154-67.
5. Choi J, Nguyen VH, Przybyszewski E, *et al.* Statin use and risk of hepatocellular carcinoma and liver fibrosis in chronic liver disease. JAMA Intern Med. 2025;185:522-30.
6. Shetty VV, Kellarai A. Comprehensive review of hepatocellular carcinoma in India: current challenges and future directions. JCO Glob Oncol. 2022. doi:10.1200/GO.22.00118.
7. Hu B, Gao Q. Global advances in hepatocellular carcinoma research and therapy in 2025. Cancer Innov. 2026;5:e70059.
8. Amin N, Anwar J, Sulaiman A, *et al.* Hepatocellular carcinoma: a comprehensive review. Diseases. 2025;13:207.
9. Foglia B, Turato C, Cannito S. Hepatocellular carcinoma: latest research in pathogenesis, detection and treatment. Int J Mol Sci. 2023;24:12224.
10. Shi H, Zou Y, Zhong W, *et al.* Complex roles of Hippo-YAP/TAZ signaling in hepatocellular carcinoma. J Cancer Res Clin Oncol. 2023;149:15311-22.
11. National Cancer Institute. Advances in liver cancer research [Internet]. Available from: https://www.cancer.gov/types/liver/research (accessed 2026 Oct 5).
12. Muddu VK, Bonda A. Hepatocellular carcinoma in India: time for a new focus. Cancer Res Stat Treat. 2023;6:449-51.
13. Pace E, Jiang Y, Clemens A, *et al.* Impact of thermal degradation of cyanidin-3-O-glucoside of haskap berry on cytotoxicity of hepatocellular carcinoma HepG2 and breast cancer MDA-MB-231 cells. Antioxidants (Basel). 2018;7:24.
14. Medic N, Tramer F, Passamonti S. Anthocyanins in colorectal cancer prevention: a systematic review of the literature in search of molecular oncotargets. Front Pharmacol. 2019;10:457301.
15. Dhivya S, Khandelwal N, Abraham SK, *et al.* Impact of anthocyanidins on mitoxantrone-induced cytotoxicity and genotoxicity: an *in vitro* and *in vivo* analysis. Integr Cancer Ther. 2016;15:525-34.
16. Yeh CT, Yen GC. Induction of apoptosis by the anthocyanidins through regulation of Bcl-2 gene and activation of c-Jun N-terminal kinase cascade in hepatoma cells. J Agric Food Chem. 2005;53:1740-9.
17. Su X, Yu H, Wang X, *et al.* Cyanidin chloride protects mice from methicillin-resistant Staphylococcus aureus-induced pneumonia by targeting Sortase A. Virulence. 2022;13:1434-45.
18. Ghosh C, Kakar R, Torkamboor S, *et al.* The regulation and function of Hippo/YAP pathway in cancer. FASEB J. 2026;40:e71744.
19. Elsori D, Pandey P, Alshaikh K, *et al.* Targeting Hippo-YAP/TAZ signaling pathway: an updated review demonstrating the therapeutic potential of key plant-derived anticancer compounds. Front Pharmacol. 2026;16:1743102.
20. Bala R, Madaan R, Bedi O, *et al.* Targeting the Hippo/YAP pathway: a promising approach for cancer therapy and beyond. MedComm (Beijing). 2025;6:e70338.
21. Shi H, Zou Y, Zhong W, *et al.* Complex roles of Hippo-YAP/TAZ signaling in hepatocellular carcinoma. J Cancer Res Clin Oncol. 2023;149:15311-22.
22. Zhang S, Zhou D. Role of the transcriptional coactivators YAP/TAZ in liver cancer. Curr Opin Cell Biol. 2019;61:64-71.
23. Lee DY, Yun SM, Song MY, *et al.* Cyanidin chloride induces apoptosis by inhibiting NF-κB signaling through activation of Nrf2 in colorectal cancer cells. Antioxidants (Basel). 2020;9:285.
24. Jia Y, Wu C, Rivera-Piza A, *et al.* Mechanism of action of cyanidin 3-O-glucoside in gluconeogenesis and oxidative stress-induced cancer cell senescence. Antioxidants (Basel). 2022;11:749.
25. Huang J, Wu L, Tashiro SI, *et al.* Reactive oxygen species mediate oridonin-induced HepG2 apoptosis through p53, MAPK, and mitochondrial signaling pathways. J Pharmacol Sci. 2008;107:370-9.
26. Granado-Serrano AB, Martín MA, Bravo L, *et al.* Quercetin induces apoptosis via caspase activation, regulation of Bcl-2, and inhibition of PI-3-kinase/Akt and ERK pathways in a human hepatoma cell line (HepG2). J Nutr. 2006;136:2715-21.
27. Lima KG, Krause GC, Schuster AD, *et al.* Gallic acid reduces cell growth by induction of apoptosis and reduction of IL-8 in HepG2 cells. Biomed Pharmacother. 2016;84:1282-90.
28. Hong L, Cai Y, Jiang M, *et al.* The Hippo signaling pathway in liver regeneration and tumorigenesis. Acta Biochim Biophys Sin (Shanghai). 2015;47:46-52.
29. Zhang J, Liu Z, Lian Z, *et al.* Monoacylglycerol lipase: a novel potential therapeutic target and prognostic indicator for hepatocellular carcinoma. Sci Rep. 2016;6:35784. doi:10.1038/srep35784.
30. Li S, Hao L, Li N, *et al.* Targeting the Hippo/YAP1 signaling pathway in hepatocellular carcinoma: from mechanisms to therapeutic drugs (review). Int J Oncol. 2024;65. doi:10.3892/ijo.2024.5676.
31. Lorthongpanich C, Charoenwongpaiboon T, Supakun P, *et al.* Fisetin inhibits osteogenic differentiation of mesenchymal stem cells via the inhibition of YAP. Antioxidants (Basel). 2021;10:879.
32. Li J, Wang H, Wang L, *et al.* Decursin inhibits the growth of HepG2 hepatocellular carcinoma cells via Hippo/YAP signaling pathway. Phytother Res. 2018;32:2456-65.

www.ijper.org

Cite this article: . Cytotoxic Effects of Cyanidin Chloride in HepG2 Cells Associated with Altered LATS1 Gene Expression. Indian J of Pharmaceutical Education and Research. 2027;1-10.